Heat Mass Transfer (2011) 47:1537–1551
DOI 10.1007/s00231-011-0814-8

ORIGINAL

Predicting the direct, diffuse, and global solar radiation on a horizontal surface and comparing with real data

M. H. Safaripour · M. A. Mehrabian

Received: 19 August 2010 / Accepted: 2 May 2011 / Published online: 19 May 2011

Abstract This paper deals with the computation of solar radiation flux at the surface of earth in locations without solar radiation measurements, but with known climatological data. Simple analytical models from literature are calibrated, and linear regression relations are developed for diffuse, and global solar radiation. The measured data for the average monthly global and diffuse irradiation in Kerman, Iran are compared to the calculated results from the existing models. The data are further compared to values calculated with a linear model using seven relevant parameters. The results show that the linear model is favoured to predict irradiation data in various parts of Iran.

List of symbols

a	Climatological constant in Eq. 1
a_w	Water vapor absorptance, Eq. 33
B_a	The percentage of diffuse radiation to the ground due to particles, Eq. 45
b	Climatological constant in Eq. 1
c	Climatological constant in Eq. 2
d	Climatological constant in Eq. 2
e	Relative error, Eq. 51
E_0	Eccentricity correction factor for the earth's orbit, Eq. 26
H	Daily global irradiation at earth's surface, Eq. 1
H_o	Extraterrestrial daily irradiation, Eq. 1
H_{DF}	Daily diffuse irradiation at earth's surface, Eq. 2
H_B	Direct daily global irradiation at earth's surface, Eq. 3
$\bar{H}$	Mean monthly global radiation flux
h	Elevation from sea level, Eq. 31
I_B	Direct beam irradiance for clear sky, Eq. 4
I_{DF}	Diffuse irradiance for clear sky, Eq. 5
I	Global Irradiance for clear sky, Eq. 6
I_o	Solar constant, Eq. 8
K^*	Constant used in Eq. 5
m	Air mass, Eq. 8
MAPE	Mean average percentage error, Eq. 53
MBD	Mean bias differences
n	Hours of measured sunshine, Eq. 1
n^*	Day of year, Eq. 26
N	Potential astronomical sunshine hours, Eq. 29
P	Local absolute pressure, Eq. 31
P_o	Reference pressure at sea level, Eq. 31
q	Coefficient in Eq. 8
r_g	Ground albedo, Eq. 44
r_s	Sky albedo, Eq. 42
R_h	Relative humidity
RMSE	Root mean square error, Eq. 52
T_A	Transmissivity due to absorption and scattering by particles, Eq. 32
T_{AA}	Transmissivity due to absorption by particles, Eq. 38
T_{AS}	Ratio of T_A to T_{AA}, Eq. 40
T_{as}	Function defined in Eq. 43
T_o	Transmissivity due to ozone, Eq. 41
T_M	Transmissivity of atmospheric gases except water vapor, Eq. 30
T_R	Transmissivity due to Rayleigh Scattering, Eq. 39
t	Test statistic
t_c	Critical value
T_{UM}	Transmissivity due to oxygen and carbon dioxide, Eq. 37
T_W	Transmissivity of water vapor, Eq. 34

M. H. Safaripour · M. A. Mehrabian (✉)
Department of Mechanical Engineering, Shahid Bahonar University of Kerman, P. O. Box 76169-133, Kerman, Iran
e-mail: ma_mehrabian@alum.mit.edu

U_W Precipitable water in a vertical column, Eq. 33
X_o The amount of ozone times the air mass, Eq. 49
α_s Solar altitude angle, Eq. 3
δ Declination angle, Eq. 28
θ Zenith angle, Eq. 5
τ_A Turbidity coefficient, Eq. 32
φ Lattitude, Eq. 25
ω Hour angle, Eq. 50
ω_s Sunset hour angle, Eq. 25

1 Introduction

The need for insolation models has been recognized for many years to properly design a solar energy system for a location lacking an insolation data base. The early and widely used insolation model was published in 1940 by Moon [1]. The Moon model predicts the direct, diffuse, and global insolation under cloudy sky conditions taking into account the water vapor absorption. This model is still used today in its original or modified forms [2, 3].

In 1978–1979 Atwater and Ball [4, 5] published their direct and global insolation models under cloudy sky conditions taking into account the water vapor and oxygen absorption. The direct insolation model was taken from Kastrov as discussed by Kondratyef [6]. The form of the equation for water vapor absorption (a_w) was taken from McDonald [7]. The value of sky albedo, $r_s = 0.0685$, for a molecular atmosphere, as reported by Lacis and Hansen [8] was used in this model. Atwater and Ball used Mie calculations to obtain turbidity coefficient, τ_A, which is much too rigorous for a simple model. Therefore, a value of τ_A that will be described later in the Bird model was used here. The input parameters required for this model are the solar constant, zenith angle, surface pressure, ground albedo, precipitable water vapor, total ozone, and broadband turbidity. The Atwater and Ball model significantly underestimates the diffuse sky irradiance. It is applicable to extremely clear atmospheric conditions with an atmospheric turbidity (base e) near 0.1 at 0.5 μm wavelength. For turbidities near 0.27, this model underestimates the global irradiance by approximately 8% for air mass 1 (AM1). This model is extremely simple but does not have a good method of treating aerosol transmittance.

A model for direct and diffuse solar insolation under cloudy sky conditions was developed by Davies and Hay [9]. The equations used in this model were particularly the result of comparing several existing models. The expressions for ozone transmittance, T_o, and water vapor absorption, a_w, were taken from Lacis and Hansen [8]. The transmission due to Rayleigh scattering, T_R, was presented in tabular form, and so the Bird model expression for T_R was used in this model. The value of aerosol transmittance, $K = 0.91$ was used for data generated in this model and is the representative of aerosol conditions in southern Ontario. The single scattering albedo, $W_o = 0.98$, and the percentage of diffuse radiation to the ground due to particles, $B_a = 0.85$, were also used in this model. The Davis and Hay model can possibly provide good agreement with the rigorous codes. However, it uses a look-up table for the Rayleigh scattering transmittance term and does not have a good method for treating aerosol transmittance. The aerosol transmittance through a vertical path used by Davis and Hay for southern Ontario ($K = 0.91$) is for an extremely clear atmosphere.

Another direct and diffuse model under cloudy sky conditions was constructed by Watt [3], based particularly on the work of Moon [1]. The upper layer broadband turbidity, τ_u, was not well defined by Watt. A value of $\tau_u = 0.02$ appears to be an average value for locations in the United States. The basic equations for direct irradiance, and solar irradiance from scattered light are given in terms of transmission functions. The Watt model is relatively complicated and appears to overestimate the global insolation for AM1 conditions by approximately 7%. This is a complete model based on meteorological parameters. However, the upper air turbidity required in this model is not readily available.

Hoyt [10] proposed a model for the calculation of solar global insolation, in which the air mass values, m, were obtained from Bemporad's [11] tables. The expression for air mass of Kasten [12] may alternatively be used in this model. The values of transmittance of aerosol scattering, T_{AS}, and transmissivity due to Rayleigh scattering, T_R, are calculated from tables furnished by Hoyt [10]. The table values from which T_{AS} is calculated are limited so that large optical depths can occur from high turbidity or from large zenith angles. The basic equations for direct irradiance, solar irradiance from atmospheric scattering, and solar irradiance from multiple reflections between the ground and sky are given in terms of transmission functions. The Hoyt model provides excellent agreement with the rigorous codes. However, its use of look-up tables and the requirement to recalculate transmittance and absorptance parameters for modified air mass values causes this model to be relatively difficult to use.

Lacis and Hansen [8] developed an extremely simple model for total downward irradiance. It tends to overestimate the global irradiance by approximately 8% at AM1, and it has no provision for calculating direct irradiance. The basic equation for global irradiance is given in terms of extraterrestrial solar irradiance and transmission functions. The Lacis and Hansen model is extremely simple.

Page [13] used the Angstrom type formula for the estimation of mean values of global radiation from sunshine

records. He derived a linear regression equation from the published observations, linking the ratio of diffuse radiation on a horizontal plane to the total radiation with the atmospheric transmission. He also proposed a method to convert the mean daily radiation on the horizontal plane to mean daily direct radiation on inclined planes using conversion factors. The Page model can estimate the diffuse radiation incident on vertical and inclined planes.

Bird and Hulstrom [14] formulated the direct insolation models. They also improved the direct irradiance models in a review evaluation study [15].

Bird and Hulstrom [16] presented a simple broadband model for direct and diffuse insolation under clear sky conditions. The model is composed of simple algebraic expressions, and the inputs to the model are from readily available meteorological data. This enables the model to be implemented very easily.

Ashjaee [17] used the Bird and Hulstrum [16] model for estimating the global irradiance in clear sky, but some modifications were done in precipitable water, U_w, and the contribution of transmissivity due to Rayleigh scattering, T_R, for calculation of diffuse component of solar radiation. On the other hand, U_w affects a_w in direct component to account for cloudiness effect. He then used the Barbaro's et al. [18] idea of the ratio of measured to astronomical sunshine duration to account for cloudiness effect.

Pisimanis and Notaridou [20] predicted the direct, diffuse, and global solar radiation on an arbitrary inclined plane in Greece. They developed a simple algorithm based on a model for insolation on clear days proposed by Bird and Hulstrom, which takes into account cloudiness variation from month to month and hour to hour. The algorithm utilizes only routine meteorological data as input and requires very limited computational resources. Its results for monthly average daily and hourly values are accurate to better than 10% in the worse case examined for global irradiation and 15% for diffuse irradiation.

Daneshyar [21] examined the various prediction methods for the mean monthly solar radiation parameters and proposed a suitable method for predicting the mean monthly values of direct, diffuse, and total solar radiation at different locations in Iran. The Daneshyar predictions for daily global irradiation as well as daily diffuse irradiation in Kerman will be compared with the predictions of linear model developed in this research.

Sabziparvar [22] revised three different radiation models (Sabbagh, Paltridge, Daneshyar) to predict the monthly average daily solar radiation on horizontal surface in various cities in central arid deserts of Iran. The modifications were made by the inclusion of altitude, monthly total number of dusty days and seasonal variation of Sun-Earth distance. He proposed a new height-dependent formula based on MBE, MABE, MPE, and RSME statistical analysis. The Sabziparvar predictions for daily global irradiation in Kerman will be compared with the predictions of linear model developed in this research.

Bahadorinejad and Mirhosseini [23] calculated the monthly mean daily clearness index for different cities in Iran. They used the SPSS statistical software and developed a relationship between the monthly mean daily clearness index (the dependent variable) and meteorological parameters such as sunshine duration ratio, relative humidity, air temperature, and daily rainfall (independent variables). They showed that in 36 cities being investigated the clearness index varied between 0.69 (for Tabas) and 0.39 (for northern coastal cities). The Bahadorinejad predictions for daily global irradiation in Kerman based on Iranian months will be compared with the predictions of linear model developed in this research.

The basic equations of the Page [13] and Bird-Hulstrom [16] models will be presented later, as these two simple models will be compared with the average monthly values of global solar radiation measured by the IMO in Kerman, the major city in the south-east region of the country. Further details regarding most of the models mentioned in this survey can be found in [16].

Since solar measurements in many Iranian cities are sparse, developing a model for accurate prediction of available solar energy in every location is worthwhile. The objective of this paper is therefore to present methods for estimating solar radiation in south-east Iran. Once these models are validated by comparing the results with the available IMO measurements in Kerman, they can be applied to locations where no measured data are available.

The aims of the present paper are: (1) calibration of two analytical models using the direct, diffuse, and global solar radiation intensities measured by the IMO in Kerman, (2) developing linear models using relevant climatological parameters, (3) using the linear models to predict the mean global solar radiation intensities in remote areas of south-east region where no measured data is available, but the model parameters can be obtained locally, and (4) showing that the linear models developed in this paper are much easier to use and give accurate results. The number of parameters needed to apply the linear models could be one, two, three, or more. Even with one parameter, the accuracy of the model is quite satisfactory.

It is worth mentioning that solar energy is abundant in Iran, especially in south-east region with hot and dry climate. The solar data in most SE areas are very close and for the major SE cities are given in Table 1.

It is expected that the application of solar energy engineering, especially solar water heaters, becomes widespread in this region in the near future. Therefore, reliable solar models to predict the global solar intensities on horizontal surfaces in remote areas of this region, in order to

Table 1 Solar data in the capitals of Kerman, Yazd, and Systan provinces

	Solar energy intensity (MJ/m^2 year)	Measured sunshine (hours/year)	Measured cloudiness (hours/year)	Lattitude (degrees)
Kerman	7,625	3,157	1,223	30.25
Yazd	7,787	3,270	1,110	31.29
Zahedan	7,645	3,241	1,139	29.47

supply the energy demands from renewable (solar) sources is of great concern.

2 Solar energy and parameter identification

Nowadays, more than 81% of the total world energy and 95% of Iran's energy consumption are provided by fossil fuels [19]. Continuation of consuming fossil fuels not only increases air, water, and soil pollution, but also results in global warming because of releasing more carbon dioxide in atmosphere. To reduce the pollution caused by using fossil fuels and optimization of oil and gas consumption in industrial and domestic sections, it is inevitable to pay more attention to solar energy which is renewable and environmentally friendly. The solar radiation energy available in Iran is tremendous and the technology to convert this energy into heat or electricity is established. According to the experimental measurements conducted by IMO the average daily solar radiation energy available in Iran is about 18 MJ/m^2 [19]. Considering the total national energy consumption in 2005 being equivalent to 1 billion oil barrels, the solar radiation energy available in an area about 0.12% of the country's land (roughly 2,000 square kilometers) would be sufficient to supply the country's total energy consumption [19]. To control and utilize such an enormous source of energy requires one to know and understand the variations and parameters influencing the solar radiation energy available in a place both quantitatively and qualitatively. This kind of information is not only used in design and assessment of solar energy systems, but also is very essential in climatology, meteorology, architecture, air conditioning, etc. The data for solar radiation energy can be obtained in two different ways. The first way which is more reliable is the direct measurement of solar radiation components. The second way relies on empirical-analytical relationships and predicts the solar radiation components as a function of time, latitude, altitude, zenith angle, clear sky conditions, hours of measured sunshine, etc. The latter can be used in locations where experimental data on solar radiation energy is scarce. To obtain a general correlation to estimate the solar radiation components taking into account all the affecting parameters, is not an easy task. On the other hand, some of the parameters are less effective and can be eliminated and only the important parameters are taken into account.

3 The page model equations

The Page model [13] predicts the mean daily solar energy intensity for cloudy sky on a horizontal surface according to the following equation:

$$H = H_0\left(a + b\frac{n}{N}\right) \tag{1}$$

The *model* equation for the monthly mean daily diffuse component is as follows:

$$\frac{\bar{H}_{\mathrm{DF}}}{\bar{H}} = c + d\frac{\bar{H}}{\bar{H}_0} \tag{2}$$

a, b, c, and d are climatologically determined constants for estimating the monthly mean daily global and diffuse radiation on a horizontal plane, their values for various localities may be found in [13]. The monthly mean values of the daily direct radiation on the horizontal plane may be found from the relation:

$$\sum H_B \sin\alpha_s = H - H_{\mathrm{DF}} \tag{3}$$

It can be shown that the maximum diffuse radiation occurs when the ratio of measured sunshine hours to potential astronomical sunshine hours, n/N, is between 40 and 50%.

The Page model (Eqs. 1–3) was calibrated using the global solar energy intensities measured by the IMO in Kerman, and the coefficients were obtained as follows:

$$a = 0.3356 \quad b = 0.4525 \quad c = 1.3434 \quad d = -1.5536$$

The details regarding the Page model are given in "Appendix A".

4 The Bird-Hulstrom model equations

The direct and diffuse components of solar radiation for cloudy sky on a horizontal surface that have been formulated by Bird and Hulstrom [16] are:

$$H_B = I_B\frac{n}{N} \tag{4}$$

$$H_{\mathrm{DF}} = I_{\mathrm{DF}}\frac{n}{N} + K^*\left(1 - \frac{n}{N}\right)(I_B + I_{\mathrm{DF}}) \tag{5}$$

$$H = (H_B\cos\theta + H_{\mathrm{DF}})/(1 - r_g r_s) \tag{6}$$

The inclusion of the ratio of measured to potential astronomical sunshine duration, n/N in the Bird-Hulstom

model accounts for the cloudiness effect. The actual average daily direct I_B, and diffuse I_{DF}, radiation in clear sky can be calculated by the following expressions [16]:

$$I_B = 0.9662 I_0 (T_M - a_w) T_A \quad (7)$$

$$I_{DF} = (I_0 \cos\theta) 0.79 T_0 T_W T_{UM} T_{AA} [q(1 - T_R) + B_a(1 - T_{AS})] / [1 - m + m^{1.02}] \quad (8)$$

T_A in Eq. 7 is a function of turbidity, while T_M and a_w are functions of pressure, air mass and precipitable water in a vertical column, U_w. The latter depends on relative humidity, temperature, and elevation from sea level. The local values for U_w in four seasons of the year starting from spring are 1, 4.5, 3, and 0.5, respectively.

This model was calibrated using the solar energy intensities and the local values of U_w measured by the IMO in Kerman and the coefficient q in Eq. 8 was obtained for estimating the hourly diffuse radiation in clear sky as follows:

$$q = 0.65$$

The details regarding the Bird-Hulstrom model [16] are given in "Appendix B".

5 Linear regression relations

The effects of geographical, geometrical, astronomical, and meteorological (GGAM) parameters on the monthly mean daily global and diffuse solar radiation in city of Kerman, south-east Iran, are studied. To fulfill this task, the measured data of global solar radiation and GGAM parameters for Kerman were used. These data were measured by Iranian Meteorological Organization (IMO) and given to the authors to conduct this research. The analysis of experimental data showed that the monthly mean daily solar radiation on a horizontal surface is related to seven GGAM parameters. These parameters are: the mean daily extraterrestrial solar radiation (H_0), the average daily ratio of sunshine duration (n/N), the mean daily relative humidity (R_h), the mean daily maximum air temperature (T_{max}), the mean daily maximum dew point temperature ($T_{dp,max}$), the mean daily atmospheric pressure (P), and sine of the solar declination angle ($\sin\delta$). Single and multiple regression relations were suggested to predict the monthly mean daily global and diffuse solar radiation on a horizontal surface in Kerman. The coefficient of correlation (R) and t statistics (t) which determine the accuracy of each relation are calculated. Relations with higher values of R and lower values of t are selected and reported in this section. Sample linear regression relations using one to seven GGAM parameters having higher values of R and lower values of t among the relations with the same number of variables are summarized in Tables 2 and 3. Table 2 specifies the relations predicting H, while Table 3 gives relations predicting H_{DF}.

6 Measured data

In this research three sets of measured data were used:

1. The data set for calibration of the Page [13] and Bird-Hulstrum [16] models.
2. The data set for new model developments.
3. The data set for cross prediction of new models.

Table 2 Linear regression relations for global solar radiation on horizontal surface for the city of Kerman

Selected variables	Regression relations	R t	Eq. no.
$\sin\delta$	$H = 20.889 + 19.711 \sin\delta$	0.95943 0.0002	9
$\sin\delta, R_h$	$H = 26.171 + 14.017 \sin\delta - 0.161 R_h$	0.97898 0.0122	10
$n/N, \sin\delta, R_h$	$H = 21.903 + 15.214 \sin\delta - 0.117 R_h + 3.939 {}^{n}/_{N}$	0.97947 0.3342	11
${}^{n}/_{N}, \sin\delta, R_h,$ $T_{dp,max}$	$H = 21.223 + 16.186 \sin\delta + 4.3212 {}^{n}/_{N}$ $- 0.116 R_h - 0.118 T_{dp,max}$	0.97972 0.0043	12
$\sin\delta, {}^{n}/_{N}, R_h,$ $T_{dp,max}, P$	$H = -23.105 + 16.760 \sin\delta + 4.442 {}^{n}/_{N}$ $- 0.112 R_h - 0.112 T_{dp,max} + 0.053 P$	0.97981 0.00001	13
$\sin\delta, {}^{n}/_{N}, R_h,$ $T_{dp,max}, P, H_0$	$H = -19.986 + 15.330 \sin\delta + 4.662 {}^{n}/_{N} - 0.109 R_h$ $- 0.111 T_{dp,max} + 0.047 P + 0.053 H_0$	0.97983 0.003	14
$H_0, \sin\delta, {}^{n}/_{N}, R_h,$ $T_{max}, T_{dp,max}, P$	$H = -23.668 + 14.723 \sin\delta + 0.0728 H_0 + 4.553 {}^{n}/_{N}$ $- 0.093 R_h + 0.036 T_{max} - 0.145 T_{dp,max} + 0.049 P$	0.97984 0.0016	15

Table 3 Linear regression relations for diffuse solar radiation on horizontal surface for the city of Kerman

Selected variables	Regression relations	R t	Eq. no.
H_0	$H_{DF} = 1.3348 + 0.1622H_0$	0.79003 0.0099	16
$^n/_N, H_0$	$H_{DF} = 6.8925 - 8.981^n/_N + 0.1905H_0$	0.94277 0.0126	17
$\sin\delta, ^n/_N, H_0$	$H_{DF} = -3.5534 - 8.9329\sin\delta - 8.5992^n/_N + 0.5144H_0$	0.95524 0.0124	18
$\sin\delta, ^n/_N, H_0,$ R_h	$H_{DF} = -9.3917 - 9.1020\sin\delta - 5.2703^n/_N$ $+ 0.5731H_0 - 0.0490R_h$	0.96104 0.0252	19
$\sin\delta, ^n/_N, H_0,$ R_h, P	$H_{DF} = -20.7720 - 8.7828\sin\delta - 5.2615^n/_N$ $+ 0.5670H_0 + 0.0499R_h + 0.0138P$	0.96112 0.0216	20
$\sin\delta, ^n/_N, H_0,$ $R_h, T_{dp,max}, P$	$H_{DF} = -21.4480 - 8.9113\sin\delta - 5.3030^n/_N$ $+ 0.5677H_0 + 0.0499R_h + 0.0147T_{dp,max} + 0.0147P$	0.96117 0.0127	21
$H_0, \sin\delta, ^n/_N, R_h,$ $T_{max}, T_{dp,max}, P$	$H_{DF} = -21.7490 - 8.9606\sin\delta - 5.3120^n/_N + 0.5694H_0$ $+ 0.0029T_{max} + 0.0513R_h + 0.0119T_{dp,max} + 0.0149P$	0.96117 0.0123	22

Table 4 A sample calculation for transmission functions on January 17 based on Bird-Hulstrom model [16] for the city of Kerman

Day hours	θ_z Eq. 50	m Eq. 35	X_0 Eq. 49	T_M Eq. 30	T_A Eq. 32	a_w Eq. 33	T_o Eq. 41	T_W Eq. 34	T_{UM} Eq. 37
6	100.3613	0	0	0	0	0	0	0	0
7	88.3389	21.4952	6.4486	0.7995	0.0334	0.1593	0.8548	0.8407	0.7543
8	77.0795	4.3865	1.316	0.9319	0.4498	0.1144	0.9531	0.8856	0.8298
9	67.001	2.5436	0.7631	0.9579	0.6148	0.1007	0.9683	0.8993	0.8505
10	58.7383	1.9206	0.5762	0.9688	0.6862	0.094	0.9741	0.906	0.8603
11	53.1617	1.6639	0.4992	0.9738	0.7186	0.0907	0.9766	0.9093	0.865
12	51.167	1.5913	0.4774	0.9753	0.7281	0.0897	0.9773	0.9103	0.8665
13	53.1617	1.6639	0.4992	0.9738	0.7186	0.0907	0.9766	0.9093	0.865
14	58.7383	1.9206	0.5762	0.9688	0.6862	0.094	0.9741	0.906	0.8603
15	67.001	2.5436	0.7631	0.9579	0.6148	0.1007	0.9683	0.8993	0.8505
16	77.0795	4.3865	1.316	0.9319	0.4498	0.1144	0.9531	0.8856	0.8298
17	88.3389	21.4952	6.4486	0.7995	0.0334	0.1593	0.8548	0.8407	0.7543
18	100.3613	0	0	0	0	0	0	0	0

The first data set consists of:

- Sunshine duration measured by Campbell-Stoke sunshine recorder for the period of 6 years.
- Global solar radiation intensity measured by pyranometer model cc-1-681 (Kipp & Zonen, Hollands) for the period of 9 years.

The second data set consists of:

1. Maximum temperature, dew point temperature, relative humidity measured for the period of 45 years (1961–2005).
2. Sunshine hours (n) measured by Campbell-Stoke sunshine recorder for the period of 41 years (1965–2005).
3. Global solar radiation intensity measured by pyranometer model cc-1-681 (Kipp & Zonen, Hollands) for the period of 22 years (1984–2005).
4. Diffuse solar radiation intensity measured by pyranometer model cc-1-681 (Kipp & Zonen, Hollands) for the period of 16 years (1990–2005).

The third data set consists of the same items listed in the second data set but for the year 2006.

The information for maximum air temperature, dew point temperature, relative humidity, the global and diffuse daily solar radiation energy, and the hours of measured sunshine as explained in the itemized data sets were borrowed from the IMO and analyzed for possible omission of erratic data. The extraterrestrial solar radiation intensity

Table 5 A sample calculation for direct, and diffuse radiation intensities on clear sky, as well as direct, diffuse, and global radiation intensities on cloudy sky on January 17 based on Bird-Hulstrom model [16] for the city of Kerman

Day hours	T_{AA} Eq. 38	T_R Eq. 39	T_{AS} Eq. 40	r_s Eq. 42	I_B MJ/m^2 Eq. 7	I_{DF} MJ/m^2 Eq. 8	H_B MJ/m^2 Eq. 4	H_{DF} MJ/m^2 Eq. 5	H MJ/m^2 Eq. 6
6	0	0	0	0	0	0	0	0	0
7	0.4835	0.2942	0.0692	0.2174	0.101809	0.0155	0.059504	0.0247	0.0276
8	0.9226	0.7247	0.4875	0.1505	1.748301	0.3025	1.021832	0.4495	0.699
9	0.9558	0.8157	0.6432	0.1256	2.50604	0.4304	1.464709	0.6421	1.2456
10	0.9662	0.8514	0.7102	0.1149	2.854271	0.4908	1.66824	0.7317	1.635
11	0.9704	0.8671	0.7405	0.11	3.017391	0.5200	1.763579	0.7743	1.8729
12	0.9716	0.8716	0.7494	0.1086	3.06599	0.5288	1.791984	0.7871	1.9532
13	0.9704	0.8671	0.7405	0.11	3.017391	0.5200	1.763579	0.7743	1.8729
14	0.9662	0.8514	0.7102	0.1149	2.854271	0.4908	1.66824	0.7317	1.635
15	0.9558	0.8157	0.6432	0.1256	2.50604	0.4304	1.464709	0.6421	1.2456
16	0.9226	0.7247	0.4875	0.1505	1.748301	0.3025	1.021832	0.4495	0.699
17	0.4835	0.2942	0.0692	0.2174	0.101809	0.0155	0.059504	0.0247	0.0276
18	0	0	0	0	0	0	0	0	0
					23.5216	4.0476	13.7477	6.0317	12.9134

Table 6 Constant parameters used in Bird-Hulstrom model [16] for the city of Kerman on January 17

δ	ω_s	q	h	P_o	P	τ_A	U_w	ϕ	n/N
−20.92°	77.121°	0.65	1754 m	101.325 Pa	74.288 Pa	0.191	0.5	30.25°	0.58
I_o	B_a	K^*	r_g						
1367	0.84	0.32	0.2						

Table 7 Sample calculations for direct, and diffuse radiation intensities on clear sky, as well as direct, diffuse, and global radiation intensities on cloudy sky in a typical day in each month based on Bird-Hulstrom model [16] for the city of Kerman

Day	n*	δ degrees	n/N	I_B MJ/m^2	I_{DF} MJ/m^2	H_B MJ/m^2	H_{DF} MJ/m^2	H MJ/m^2
Jan. 17	17	−20.917	0.58	23.5216	4.1368	13.6425	6.0316	12.9135
Feb. 16	47	−12.955	0.79	27.1798	4.7968	21.4720	5.8636	17.8822
Mar. 16	75	−2.418	0.65	30.221	5.3501	19.6436	7.383	20.043
Apr. 15	105	9.415	0.65	33.7797	5.9901	21.9568	8.2392	23.7966
May 15	135	18.792	0.76	36.4533	6.4703	27.7045	8.081	28.4269
Jun. 11	162	23.086	0.73	35.6186	6.3316	26.0015	8.1049	27.575
Jul. 17	198	21.184	0.76	35.2505	6.2664	26.7903	7.8193	27.6989
Aug. 16	228	13.455	0.83	33.3893	5.9344	27.7131	6.9762	26.7699
Sep. 15	258	2.217	0.78	30.3745	5.3776	23.6921	6.5953	22.6739
Oct. 15	288	−9.599	0.78	26.9811	4.7754	21.0452	5.8784	18.2554
Nov. 14	318	−18.912	0.78	23.1099	4.0797	18.0257	5.0086	14.3254
Dec. 10	344	−23.050	0.62	22.5894	3.9708	14.0054	5.6383	12.3131

(H_0), solar declination angle (δ), and the potential astronomical sunshine hours (N) were calculated from Eqs. 25, 28, and 29 respectively.

The global/diffuse solar radiation intensities in three sets of data described above were instantaneously measured every day at Kerman International Airport and integrated over the sunshine duration to obtain the mean daily values.

7 Results

Two existing radiation models mentioned in this paper were calibrated and validated to estimate the solar radiation distribution in Kerman province. The calibration was performed using the diffuse and global solar radiation intensities measured by the IMO in the city of Kerman.

Table 8 Sample calculations for direct, diffuse, and global radiation intensities on cloudy sky in a typical day in each month based on Page model [13] for the city of Kerman

Day	n*	δ degrees	n/N	ω_s	E_o	H_o MJ/m^2	H_{DF} MJ/m^2	H MJ/m^2
Jan. 17	17	−20.917	0.58	77.12106	1.0316	21.1185	5.0011	13.05317
Feb. 16	47	−12.955	0.79	82.29048	1.0228	25.84096	4.3402	18.42709
Mar. 16	75	−2.418	0.65	88.58905	1.0091	31.48631	6.8318	20.45854
Apr. 15	105	9.415	0.65	95.54921	0.9923	36.76829	7.9778	23.89057
May 15	135	18.792	0.76	101.4457	0.9774	40.01172	7.1826	27.98916
Jun. 11	162	23.086	0.73	104.3934	0.9690	41.1533	7.8394	28.22919
Jul. 17	198	21.184	0.76	103.0624	0.9682	40.47782	7.2662	28.31521
Aug. 16	228	13.455	0.83	98.02049	0.9766	37.90724	5.7492	27.71747
Sep. 15	258	2.217	0.78	91.29378	0.9912	33.31392	5.7258	23.60531
Oct. 15	288	−9.599	0.78	84.33983	1.0080	27.43452	4.7153	19.43933
Nov. 14	318	−18.912	0.78	78.47471	1.0228	22.19031	3.8140	15.72344
Dec. 10	344	−23.050	0.62	75.63254	1.0309	19.752	4.4612	12.56599

Table 9 Monthly solar gain (H and H_{DF}) distribution based on linear model with 7 parameters for the city of Kerman

n*	δ degrees	n/N	H_o MJ/m^2/day	T_{max} °C	R_h	$T_{dp,max}$ °C	P mbar	H MJ/m^2/day	H_{DF} MJ/m^2/day
17	−20.92	0.58	21.12	11.73	52.58	−5.70	833.07	12.41	5.44
47	−12.95	0.79	25.84	12.70	41.59	−8.06	832.36	17	5.26
75	−2.42	0.65	31.49	16.73	43.60	−3.70	832.21	18.77	7.75
105	9.41	0.65	36.77	23.89	30.98	−2.99	832.21	23.53	8.28
135	18.79	0.76	40.01	28.58	24.86	−1.68	831.75	27.13	7.82
162	23.09	0.73	41.15	33.03	19.45	−0.85	829.32	28.55	7.70
198	21.18	0.76	40.48	34.09	19.10	0.87	827.18	27.89	7.42
228	13.45	0.83	37.91	33.20	19.09	−0.60	829.13	26.38	6.78
258	2.22	0.78	33.31	30.22	20.65	−2.47	832.34	23.16	6.23
288	−9.60	0.78	27.43	23.87	28.49	−4.02	836.25	19.15	5.17
318	−18.91	0.78	22.19	17.77	41.82	−3.74	836.61	14.98	4.25
344	−23.05	0.62	19.75	13.65	47.69	−6.51	835.67	12.72	4.58

A sample calculation for a typical day (January 17) is carried out on an hourly basis in Tables 4, 5 and 6. Table 4 accounts for transmission functions. Table 5 accounts for the mean hourly radiation components on a clear sky as well as on a cloudy sky. The mean daily radiation components on a clear sky as well as on a cloudy sky are listed in the last row of Table 5 as the sum of hourly values for corresponding column. Table 6 gives the parameters which are constant over the daily hours. Similar calculations as those conducted for a typical day in January, are carried out for a typical day in other months. The results are reported in Table 7. Sample calculations for direct, diffuse, and global radiation intensities on cloudy sky in a typical day in each month based on the Page model [13] for the city of Kerman are presented in Table 8. Table 9 gives the monthly solar gain (H and H_{DF}) distribution based on linear regression relation with seven parameters for the city of Kerman. Tables 10 and 11 respectively present the error analysis for predictions of linear models for global and diffuse solar radiation. The global and diffuse solar radiation intensities predicted by regression relations for the city of Kerman are shown in Figs. 1 and 2 respectively. These models can be used in small towns and villages in the province, where a meteorological station does not exist, and thus, direct measurement of solar radiation intensity is not possible.

The global and diffuse solar radiation intensities predicted by the Page [13] and Bird-Hulstrom [16] models for the city of Kerman are shown in Figs. 1 and 2, respectively. The model predictions are compared with the corresponding measured data. The error analysis was performed for the Page [13] and Bird-Hulstrom [16] models when compared with corresponding measured data. The models predicted the global and diffuse solar radiation intensities and the relative errors are shown in Tables 12 and 13, respectively.

Table 10 Error analysis for linear model predictions of H (MJ/m^2/day)—relative errors (%) against real data

Month	Data (H)	Eq. 9 e (%)	Eq. 10 e (%)	Eq. 11 e (%)	Eq. 12 e (%)	Eq. 13 e (%)	Eq. 14 e (%)	Eq. 15 e (%)
Jan	12.52	10.86	0.08	0.80	0.56	0.16	0.08	0.16
Feb	15.83	3.28	−1.26	−1.20	−0.25	−0.69	−0.51	−0.63
Mar	18.38	9.19	2.29	1.47	1.52	1.47	1.80	1.74
Apr	23	4.96	0.22	−0.48	−0.48	−0.13	−0.04	−0.04
May	26.83	1.53	−1.27	−1.04	−0.82	−0.37	−0.45	−0.45
Jun	28.54	0.28	0.42	0.56	1.05	0.98	0.81	0.84
Jul	28.1	−0.43	−0.04	−0.11	−0.60	−0.96	−1.07	−1.10
Aug	25.9	−1.85	1.12	1.78	1.35	1.08	1.20	1.20
Sep	23.58	−8.52	−1.19	−1.31	−1.27	−1.31	−1.15	−1.02
Oct	19.32	−9.32	−0.36	−0.52	−0.67	−0.26	−0.16	−0.16
Nov	15.2	−4.87	2.43	2.50	2.37	2.70	2.50	2.37
Dec	13.19	−0.23	−2.65	−2.58	−2.88	−2.96	−3.34	−3.26
MBD		−0.0001	0.0009	0.0012	−0.0003	0	−0.0002	−0.0001
RMSE		1.0978	0.2521	0.2598	0.2527	0.2485	0.2537	0.2501
t		0.0002	0.0124	0.0156	0.0043	0.0001	0.0032	0.0017
Tc		2.2010	2.2010	2.2010	2.2010	2.2010	2.2010	2.2010

Table 11 Error analysis for linear model predictions of H_{DF} (MJ/m^2/day)—relative errors (%) against real data

Month	Data (HDF)	Eq. 16 e (%)	Eq. 17 e (%)	Eq. 18 e (%)	Eq. 19 e (%)	Eq. 20 e (%)	Eq. 21 e (%)	Eq. 22 e (%)
Jan	5.23	−8.8	3.06	−0.38	2.29	2.1	2.29	2.29
Feb	6.14	−10.59	−3.42	−0.81	0.65	0.33	0	0
Mar	8.06	−20.1	−5.71	−1.49	−1.12	−1.24	−1.24	−1.24
Apr	8.6	−15.12	−2.79	−0.23	−0.35	−0.12	−0.12	−0.12
May	8.16	−4.17	−0.25	−1.47	−0.37	0	0	0
Jun	7.46	7.37	5.36	0.8	0.4	0.4	0.27	0.27
Jul	7.41	6.61	5.94	2.29	1.21	0.94	1.21	1.08
Aug	6.88	8.58	−4.07	−3.05	−1.74	−2.03	−1.89	−1.89
Sep	5.86	14.68	−2.22	2.9	1.19	1.02	1.02	1.02
Oct	4.92	17.07	−3.05	1.42	−1.02	−0.61	−0.61	−0.61
Nov	3.98	23.62	5.28	3.27	1.01	1.26	1.51	1.51
Dec	4.44	2.25	6.08	−0.68	−1.35	−1.35	−1.35	−1.13
MBD		0.0025	0.0011	−0.0004	−0.0005	−0.0005	−0.0003	−0.0003
RMSE		0.8321	0.2791	0.1174	0.0722	0.0707	0.0697	0.0697
t		0.0099	0.0126	0.0124	0.0252	0.0216	0.0127	0.0123
Tc		2.201	2.201	2.201	2.201	2.201	2.201	2.201

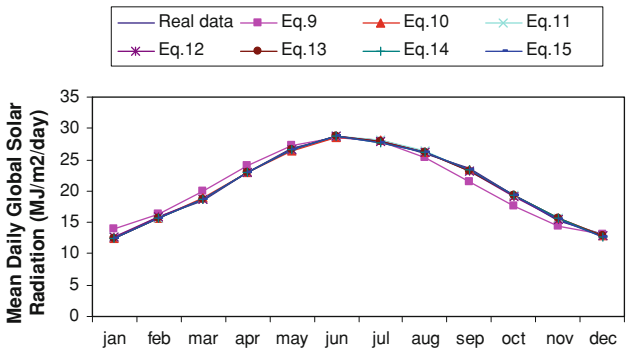

Fig. 1 Linear model predictions for $\bar{H}$ compared with real data

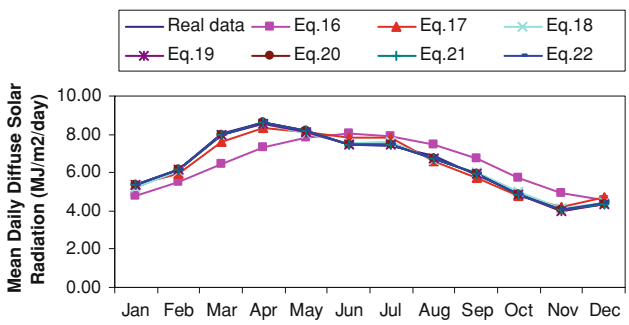

Fig. 2 Linear model predictions for $\bar{H}_{DF}$ compared with real data

Table 12 Error analysis for Bird-Hulstrom [16], Page [13], Sabziparvar [22], Daneshyar [21], and linear model predictions of H (MJ/m^2/day)—relative errors (%) against real data

Month	Bird-Hulstrom [16] model		Page [13] model		Sabziparvar [22]		Daneshyar [21]		Linear model, Eq. 15		Real data
	H	e (%)	H	e (%)	H	e (%)	H	e (%)	H	e (%)	
January	13.15	5.06	13	3.81	13.03	4.07	10.75	−14.14	12.54	0.15	12.52
February	16.41	3.64	16.1	1.71	14.96	−5.5	14.04	−11.31	15.73	−0.63	15.83
March	19.27	4.84	18.93	2.94	16.24	−11.64	17.43	−5.17	18.7	1.71	18.38
April	23.22	0.93	22.6	−1.76	19.13	−16.83	19.84	−13.74	22.99	−0.06	23
May	27.43	2.22	26.27	−2.08	23.75	−11.48	24.49	−8.72	26.71	−0.45	26.83
June	28.15	−1.34	28.04	−1.73	28.51	−0.11	26.99	−5.43	28.78	0.85	28.54
July	27.45	−2.32	27.32	−2.8	29.99	6.73	26.52	−5.62	27.79	−1.12	28.1
August	26.82	3.56	26.96	4.09	28.99	11.93	25.3	−2.32	26.21	1.19	25.9
September	23.29	−1.23	23.62	0.16	27.71	17.51	21.83	−7.42	23.34	−1.03	23.58
October	18.46	−4.44	19.18	−0.71	20.14	4.24	17.3	−10.46	19.29	−0.14	19.32
November	14.19	−6.69	15.11	−0.62	15.89	4.54	13.16	−13.42	15.56	2.35	15.2
December	12.55	−4.79	12.53	−4.96	12.56	−4.78	10.58	−19.79	12.76	−3.24	13.19
MAPE	3.42		2.28		8.28		9.79		1.08		
RMSE	0.68		0.54		2.27		1.96		0.25		

Table 13 Error analysis for Bird-Hulstrom [16], Page [13], Daneshyar [21], and linear model prediction for H_{DF} (MJ/m^2/day)—Relative errors (%) against real data

Month	Bird-Hulstrom [16] model		Page [13] model		Daneshyar [21]		Linear model Eq. 22		Real data
	HDF	e (%)	HDF	e (%)	HDF	e (%)	HDF	e (%)	
Jan	5.89	12.71	5.29	1.12	3.63	−30.59	5.35	2.29	5.23
Feb	6.57	7.05	6.2	0.97	4.23	−31.11	6.14	0	6.14
Mar	7.82	−2.95	8.02	−0.5	4.91	−39.08	7.96	−1.24	8.06
Apr	8.48	−1.45	8.55	−0.62	6.26	−27.21	8.59	−0.12	8.6
May	8.46	3.69	8.09	−0.84	6.09	−25.37	8.16	0	8.16
Jun	7.88	5.68	7.59	1.72	6.09	−18.36	7.48	0.27	7.46
Jul	7.9	6.56	7.44	0.36	5.88	−20.65	7.49	1.08	7.41
Aug	6.9	0.33	7.3	6.15	5.29	−23.11	6.75	−1.89	6.88
Sep	6.29	7.33	5.74	−1.97	4.44	−24.23	5.92	1.02	5.86
Oct	5.69	15.75	4.81	−2.17	3.81	−22.56	4.89	−0.61	4.92
Nov	5.06	27.01	4.24	6.63	3.09	−22.36	4.04	1.51	3.98
Dec	5.43	22.33	4.03	−9.15	3.17	−28.6	4.39	−1.13	4.44
MAPE	9.4		2.68		26.1		0.93		
RMSE	0.59		0.2		1.79		0.07		

8 Comparison and discussion

The mean daily global radiation intensities predicted by the regression relations with one (Eq. 9) to seven (Eq. 15) relations are compared with real data in Fig. 3. The figure is an indication of the fact that a better agreement between the predicted values and real data is achieved, as the number of variables in the regression relation is increased. The relation with seven variables (Eq. 15) is therefore chosen to be compared with analytical models.

The mean daily diffuse radiation intensities predicted by the regression relations with one (Eq. 16) to seven (Eq. 22) relations are compared with real data in Fig. 4. The figure is an indication of the fact that a better agreement between the predicted values and real data is achieved, as the number of variables in the regression relation is increased. The relation with seven variables (Eq. 22) is therefore chosen to be compared with analytical models.

The global radiation results predicted by the Page [13] and Bird-Hulstrom [16] models for the city of Kerman, as

well as the predictions of Eq. 15 are compared with measured data in Fig. 3. Both Page and Bird-Hulstrom models are less accurate than Eq. 15, but the Page [13] model predictions, however, have less deviation from the measured data.

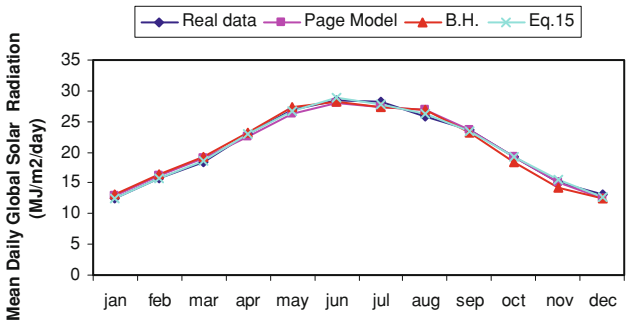

Fig. 3 Bird-Hulstrom [16], Page [13], and linear model predictions for $\bar{H}$ compared with real data

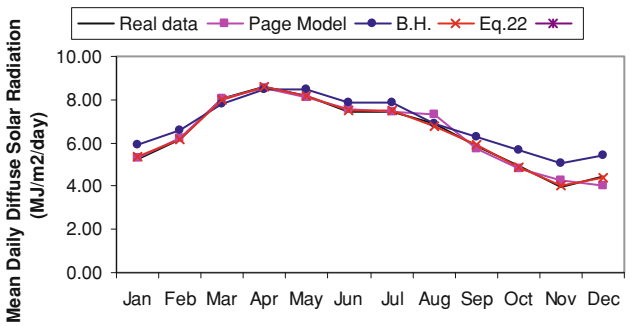

Fig. 4 Bird-Hulstrom [16], Page [13], and linear model predictions for $\bar{H}_{DF}$ compared with real data

The diffuse radiation results predicted by the Page [13] and Bird-Hulstrom [16] models for the city of Kerman, as well as the predictions of Eq. 22 are compared with measured data in Fig. 4. Both Page and Bird-Hulstrom models are less accurate than Eq. 22, but the Page [13] model predictions, however, have less deviation from the measured data.

The relative errors for the predicted results (the global solar radiation) are reported in Table 12. The biggest error for the Page [13] model happens in December (4.96% underestimation), and the smallest error for this model happens in September (0.16% overestimation). The biggest error for the Bird-Hulstrom [16] model happens in November (6.69% underestimation), while the smallest error for this model happens in April (0.93% overestimation). The biggest error for the linear model (Eq. 15) happens in December (3.24% underestimation), while the smallest error happens in April (0.06% underestimation).

The relative errors for the predicted results (the diffuse solar radiation) are reported in Table 13. The biggest error for the Page [13] model happens in December (9.15% underestimation), and the smallest error for this model happens in July (0.36% overestimation). The biggest error for the Bird-Hulstrom [16] model happens in November (27.01% overestimation), while the smallest error for this model happens in April (0.33% overestimation). The biggest error for the linear model (Eq. 22) happens in January (2.29% overestimation), while the smallest error happens in February and May (0.00%).

Table 14 Error analysis for Page, Bird-Hulstrom [16], Bahadorinejad [23], and linear model (Eq. 15) for H (MJ/m^2/day) based on Iranian months—Relative errors (%) against real data

Month	Bird-Hulstrom [16] model		Page [13] model		Bahadorinejad [23]		Linear model Eq. 22		Real data
	H	e (%)	H	e (%)	H	e (%)	H	e (%)	
Far.	23.22	0.96	22.6	−1.74	21.52	−6.43	22.99	−0.04	23
Ord.	27.43	2.24	26.27	−2.09	25.13	−6.34	26.71	−0.45	26.83
Kho.	28.15	−1.37	28.04	−1.75	27.47	−3.75	28.78	0.84	28.54
Tir	27.45	−2.31	27.32	−2.78	28.56	1.64	27.79	−1.1	28.1
Mor.	26.82	3.55	26.96	4.09	27.48	6.1	26.21	1.2	25.9
Sha.	23.29	−1.23	23.62	0.17	24.14	2.37	23.34	−1.02	23.58
Meh.	18.46	−4.45	19.18	−0.72	19.54	1.14	19.29	−0.16	19.32
Aba.	14.19	−6.64	15.11	−0.59	15.12	−0.53	15.56	2.37	15.2
Aza.	12.55	−4.85	12.53	−5	12.22	−7.35	12.76	−3.26	13.19
Day	13.15	5.03	13	3.83	11.37	−9.19	12.54	0.16	12.52
Bah	16.41	3.66	16.1	1.71	14.17	−10.49	15.73	−0.63	15.83
Esf.	19.27	4.84	18.93	2.99	16.91	−8	18.7	1.74	18.38
MAPE	3.43		2.29		5.28		1.08		
RMSE	0.68		0.54		1.17		0.25		

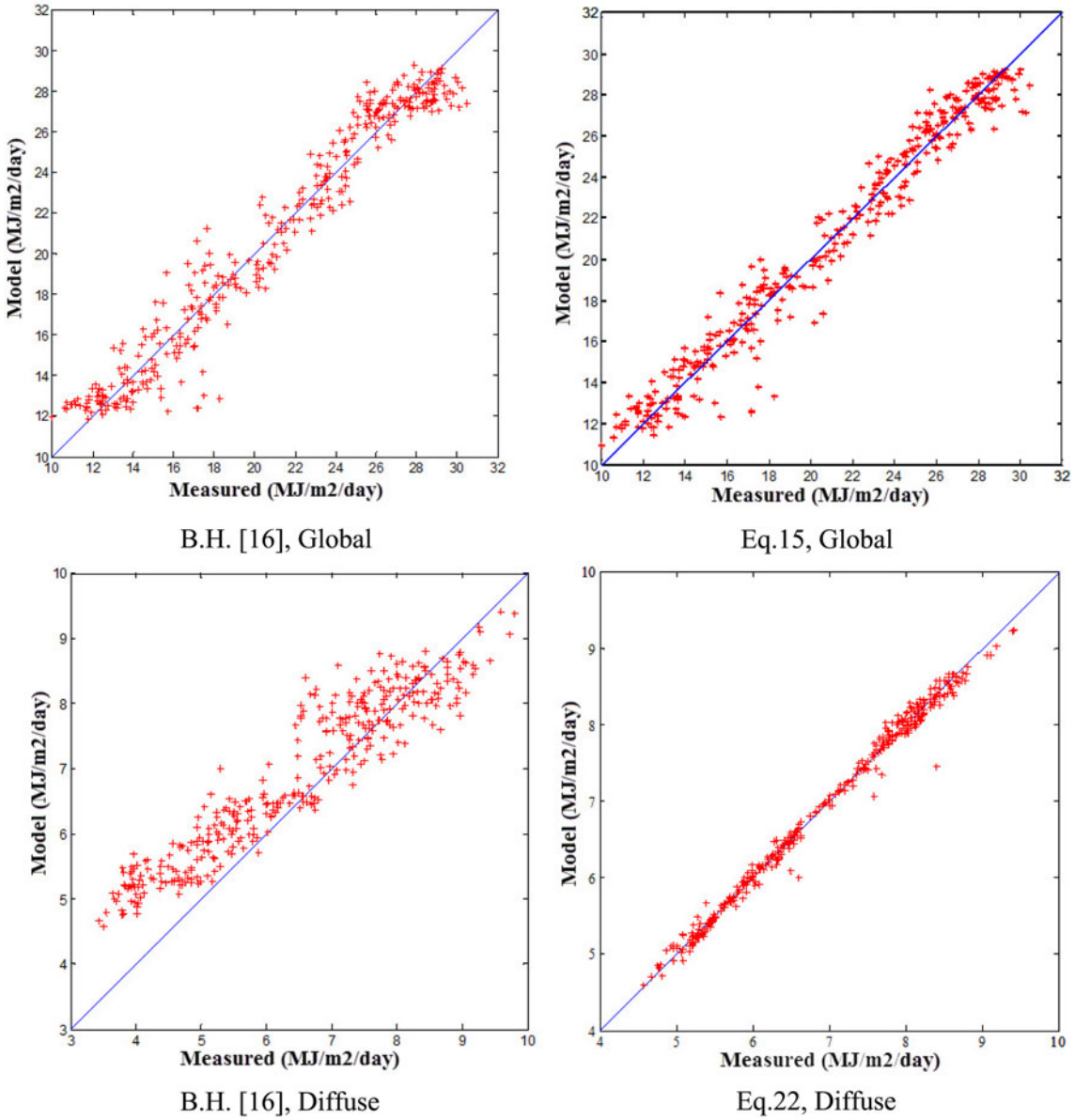

Fig. 5 Scatter plots for global and diffuse solar radiation based on mean daily values

The predictions of the Page [13], Bird-Hulstrom [16], and Bahadorinejad [23] models for the city of Kerman, together with the measured data for this city are listed in Table 14. This comparison has been carried out with respect to the Iranian months rather than Christian months. The mean average percentage errors as well as the root mean square error for each model have been calculated and reported in the table. The mean average percentage errors for these models are 2.29, 3.43, and 5.28%, respectively. The RSME for the above models are 0.54, 0.68, and 1.17, respectively. This comparison indicates that the modified Page [13] model offers closer results to the measured data. The definitions for the mean relative error (e), root mean square error (RMSE), and mean average percentage error (MAPE) are given in "Appendix C".

The scatter plots of measured data for the city of Kerman versus the predictions of modified Page [13] and Bird-Hulstrom [16] models as well as the regression equations with seven parameters are shown in Figs. 5 and 6. Figure 5 is based on the mean daily values, while Fig. 6 is based on the mean monthly values.

9 Validation of results and cross prediction of data

The regression relations listed in Table 2 are based on independent variables measured on a daily basis, data set 2.

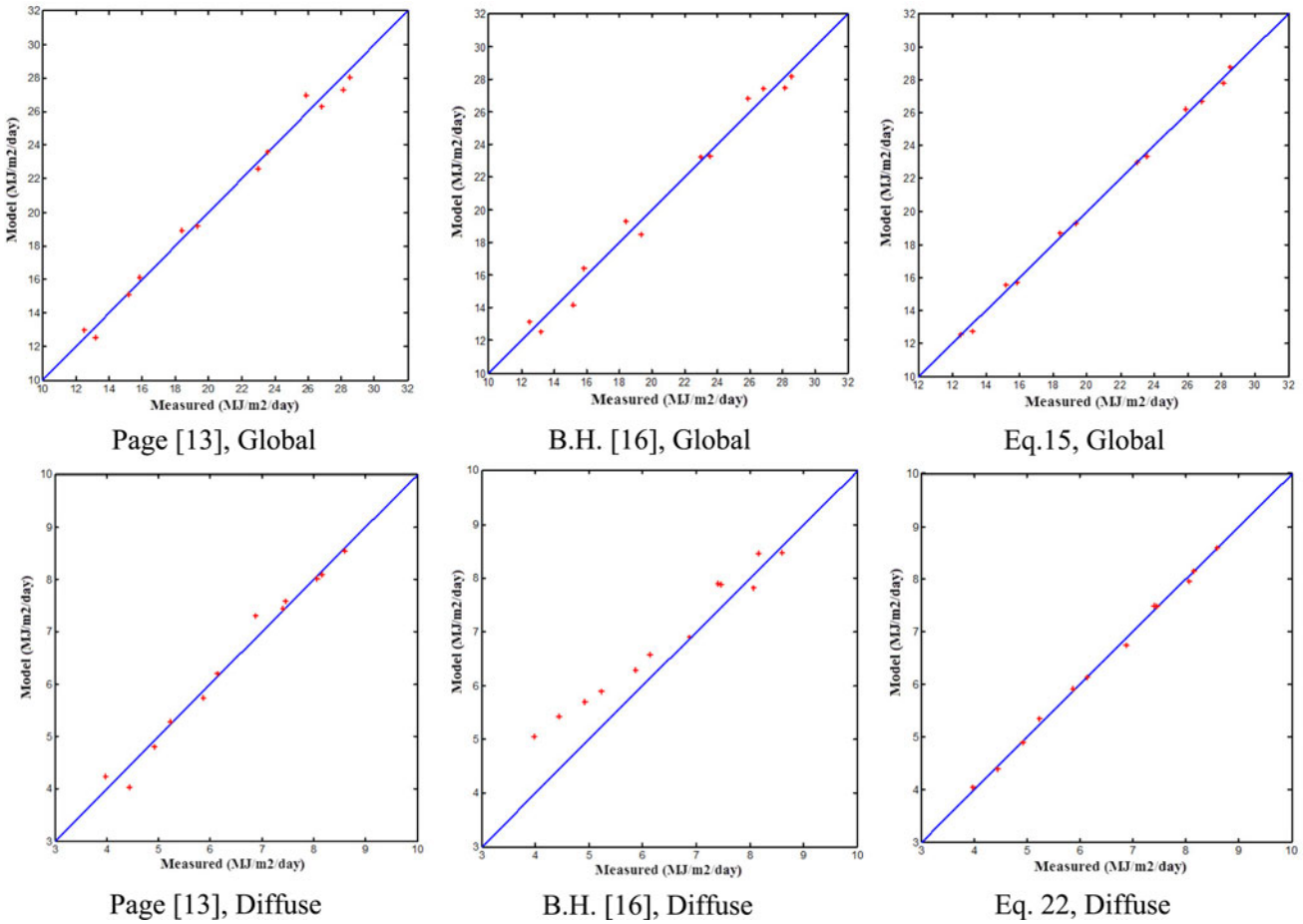

Fig. 6 Scatter plots for global and diffuse solar radiation based on mean monthly values

A dummy variable investigation is carried out with the independent variables based on mean monthly values, extracted from data set 3. The resulting regression relation when seven variables are involved is:

$$\bar{H} = 19.109 + 10.0483\sin\bar{\delta} + 0.24\bar{H}_0 + 10.6494\bar{n}/\bar{N} - 0.0462\bar{R}_h - 0.0886\bar{T}_{\max} - 0.0705\bar{T}_{\mathrm{dp,max}} - 0.0152\bar{P} \quad (23)$$

The global solar radiation intensities predicted by Eqs. 22, 23, and the measured data are plotted in Fig. 7. The IMO set of data used in Fig. 7 are selected at mid day of each month. Figure 7 shows that Eq. 23 (dummy variable) gives more accurate results.

The data resulting in Eqs. 9–22 are the mean daily values over a 22 year period (data set 2). In order to examine whether or not the coefficients in regression equation are constant over time, the data in a 1 year period (data set 3) were used to develop a regression relation based on seven independent variables. The new equation turned out to be:

$$H = -40.3141 + 7.9617\sin\delta + 0.3097H_0 + 10.8808n/N - 0.0144R_h - 0.0076T_{\max} - 0.1226T_{\mathrm{dp,max}} + 0.0501P \quad (24)$$

Comparing Eq. 24 with Eq. 22 shows that regression coefficients vary over time. The global solar radiation intensities predicted by Eqs. 24, 22, and measured data at mid day of each month are plotted in Fig. 8.

10 Conclusions

The Page model [13] was modified to fit the global solar radiation intensities measured in Kerman. The coefficients a and b in the model equation for the mean daily global solar energy turned out to be 0.3356 and 0.4525, respectively. A thorough consideration makes it evident that the modified model is valid for all parts of Kerman, Yazd, and Systan provinces, provided the coefficient a is expressed in

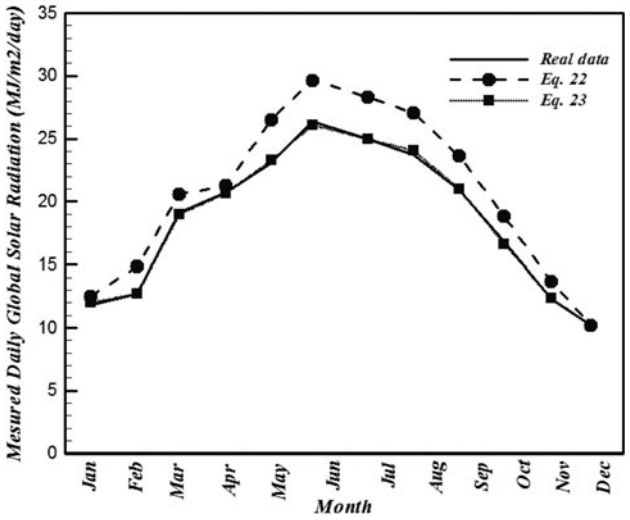

Fig. 7 Comparison of measured and estimated values using Eqs. 22 and 23

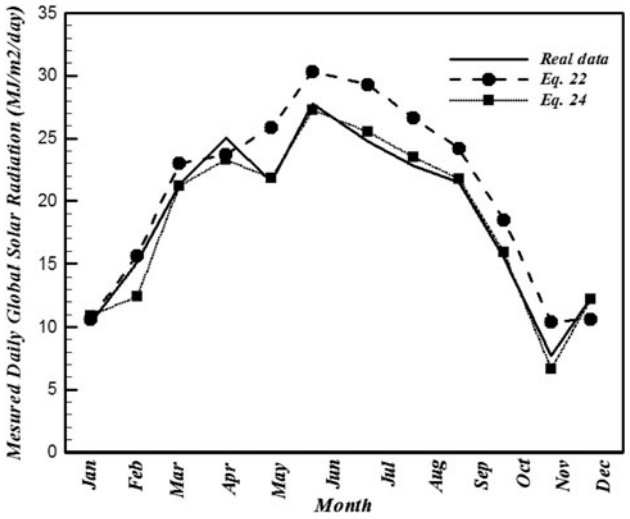

Fig. 8 Comparison of measured and estimated values using Eqs. 22 and 24

terms of latitude of the area under consideration according to the following relationship:

$$a = 0.4013 \cos \varphi$$

In the city of Kerman, for which $\varphi = 30.25°$, the value of a would be 0.3356. The φ values for other two major SE cities are given in Table 1.

The Bird-Hulstrom [16] model was modified to fit the global solar radiation intensities measured in Kerman. The local values for U_w in four seasons of the year starting from spring are 1, 4.5, 3, and 0.5, respectively. The coefficient q turned out to be 0.65. The modified model is valid for all parts of Kerman, Yazd, and Systan provinces, provided the right geographical parameters (such as h, θ,…) for the selected area are included in the model equations.

The modified Page [13] and Bird-Hulstrom [16] models, when calibrated, were in good agreement with the global solar radiation intensities measured in Yazd and Zahedan. The modified models can therefore be applied in remote regions of the three provinces where no measured data are available. To verify the validity of the modified models, their predictions were compared with the measured data in the capital cities of three provinces.

Linear regression relations are developed to predict the diffuse, and global radiation intensities on a horizontal surface. The results are compared with the average monthly values of corresponding solar radiation components measured by IMO. The strict correspondence between the model values and the real data makes the regression models a viable tool for those locations in SE Iran where no measured data on solar radiation are available.

Acknowledgments The authors would like to express their gratitude to the Iranian Meteorological Organization (IMO) for their sincere cooperation in providing the files and documents available in their archive containing meteorological information regarding Kerman airport station. Without this information this research would have not been successful. The authors also extend their appreciation to Mr. Pouyan Talbizadeh, the graduate student at SBUK, for his sincere support and encouragement.

Appendix A

$$H_0 = \frac{24 I_0 E_0}{\pi}(\cos\varphi \cos\delta \sin\omega_s + \frac{\pi\omega_s}{180}\sin\varphi \sin\delta) \quad (25)$$

$$E_0 = \left(1 + 0.033 \cos\frac{360 n^*}{365}\right) \quad (26)$$

$$\omega_s = \cos^{-1}(-\tan\varphi \tan\delta) \quad (27)$$

$$\delta = 23.45 \sin\left(360\frac{284 + n^*}{365}\right) \quad (28)$$

$$N = \frac{2\omega_s}{15} \quad (29)$$

Appendix B

$$T_M = 1.041 - 0.15[m(9.368 * 10^{-4} P + 0.051)]^{\frac{1}{2}} \quad (30)$$

$$\frac{P}{P_0} = \exp\left(\frac{h}{1000(-0.174 - 0.0000017h)}\right) \quad (31)$$

$$T_A = \exp(-\tau_A^{0.873}(1 + \tau_A - \tau_A^{0.7088})m^{0.9108}) \quad (32)$$

$$a_w = 2.4959mU_w\left[(1.0 + 79.03mU_w)^{0.6824} + 6.385mU_w\right]^{-1} \quad (33)$$

$$T_w = 1 - a_w \quad (34)$$

$$m = 1/\left[\cos\theta + 0.15(93.885 - \theta)^{-1.253}\right] \quad (35)$$

$$\tau_A = 0.2758\tau_{A(0.38)} + 0.35\tau_{A(0.50)} \quad (36)$$

$$T_{UM} = \exp(-0.127m^{0.26}) \quad (37)$$

$$T_{AA} = 1 - 0.1(1 - T_A)(1 - m + m^{1.06})) \quad (38)$$

$$T_R = \exp(-0.093m^{0.84}) \quad (39)$$

$$T_{AS} = T_A/T_{AA} \quad (40)$$

$$T_0 = 1 - 0.161X_0(1 + 139.48X_0)^{-0.3035} - \frac{0.00271X_0}{1.0 + 0.0044X_0 + 0.0003X_0^2} \quad (41)$$

$$r_s = 0.0685 + (1 - B_a)(1 - T_{as}) \quad (42)$$

$$T_{as} = 10^{-0.045[(P/P_0)m]^{0.7}} \quad (43)$$

$$r_g = 0.2 \quad (44)$$

$$B_a = 0.84 \quad (45)$$

$$K^* = 0.32 \quad (46)$$

$$\tau_{A(0.38\mu m)} = 0.35 \quad (47)$$

$$\tau_{A(0.50\mu m)} = 0.27 \quad (48)$$

$$X_0 = 0.3m \quad (49)$$

$$\cos\theta = \cos\phi\cos\delta\cos\omega + \sin\phi\sin\delta \quad (50)$$

Appendix C

$$e = \frac{H_{i,m} - H_{i,c}}{H_{i,m}} \times 100 \quad (51)$$

$$\mathrm{RMSE} = \left[\frac{1}{n}\sum_{i=1}^{n}\left(H_{i,m} - H_{i,c}\right)^2\right]^{1/2} \quad (52)$$

$$\mathrm{MAPE} = \frac{100}{n}\sum_{i=1}^{n}\left|\frac{H_{i,m} - H_{i,c}}{H_{i,m}}\right| \quad (53)$$

References

1. Moon P (1940) Proposed standard solar-radiation curves for engineering use. J Frankl Inst 230:583–617
2. Mahaptra AK (1973) An evaluation of a spectro-radiometer for the visible-ultraviolet and near-ultraviolet. Ph.D. dissertation; University of Missouri; Columbia, Mo, p 121 (University Microfilms 74-9964)
3. Watt D (1978) On the nature and distribution of solar radiation. HCP/T2552-01. U.S. Department of Energy
4. Atwater MA, Ball JT (1978) A numerical solar radiation model based on standard meteorological observation. Sol Energy 21:163–170
5. Atwater MA, Ball JT (1979) Sol Energy 23:725
6. Kondratyev KY (1969) Radiation in the atmosphere. Academic press, New York
7. McDonald JE (1960) Direct absorption of solar radiation by atmospheric water vapor. J Metrol 17:319–328
8. Lacis AL, Hansen JE (1974) A parameterization for absorption of solar radiation in the earth's atmosphere. J Atmospheric Sci 31:118–133
9. Davies JA, Hay JE (1979) Calculation of the solar radiation incident on a horizontal surface. In: Proceedings, first Canadian solar radiation data workshop, 17–19 April 1978. Canadian Atmospheric Environment Service
10. Hoyt DV (1978) A model for the calculation of solar global insolation. Sol Energy 21:27–35
11. Bemporad A (1904) Zur Theorie der Extinktion des Lichtes in der Erd-atmosphare Mitteilungen der Grossherzoglichen Sternmwarte Zu Heidel-berg; No. 4
12. Kasten F (1964) A new table and approximation formula for the relative optical air mass. Thechnical Report 136, Hanover, New Hampshire: U. S. Army Material Command, Cold Region Research and Engineering Laboratory
13. Page JK (1964) The estimation of monthly mean values of daily total short—wave radiation on vertical and inclined surfaces from sunshine records for latitude 40°N–40°S. Sol Energy 10:119
14. Bird RE, Hulstrom RE (1980) Direct insolation models. SERI/TR-335–344. Solar Energy Research Institute, Golden
15. Bird RE, Hulstrom RE (1981) Review evaluation and improvement of direct irradiance models. J Sol Energy Eng 103:183
16. Bird RE, Hulstrom RE (1981) A simplified clear sky model for direct and diffuse insolation on horizontal surface, U. S. Solar Energy Research Institute (SERI), Technical Report TR-642-761, Golden, Colorado
17. Ashjaee M, Roomina MR, Ghafouri-Azar R (1993) Estimating direct, diffuse, and global solar radiation for various cities in Iran by two methods and their comparison with the measured data. Sol Energy 50(5):441–446
18. Barbaro S, Coppolino S, Leone C, Sinagra E (1979) An atmospheric model for computing direct and diffuse solar radiation. Sol Energy 22:225–228
19. Saffaripour MH (2009) Study of influencing parameters and developing meteorological models for solar energy gain in a dry and hot region of Iran including five provinces. Ph. D. dissertation, Department of Mechanicl Engineering, Shahid Bahonar University of Kerman, May 2009
20. Pisimanis D, Notaridou V (1987) Estimating direct, diffuse and global solar radiation on an arbitrary inclined plane in Greece. Sol Energy 39:159–172
21. Daneshyar M (1978) Solar radiation statistics for Iran. Sol Energy 21:345–349
22. Sabziparvar AA (2008) A simple formula for estimating global solar radiation in central arid deserts of Iran. Renew Energy 33(5):1002–1010
23. Bahadorinejad M, Mirhosseini SA (2004) Clearness index data for various cities in Iran. Presented at the third conference on optimization of fuel consumption in building, persion volume, pp 603–619